The Astrophysical Journal, 646: L13–L16, 2006 July 20
© 2006. The American Astronomical Society. All rights reserved. Printed in U.S.A.

THE *XMM* CLUSTER SURVEY: A MASSIVE GALAXY CLUSTER AT $z = 1.45$

S. A. Stanford,[1,2] A. Kathy Romer,[3] Kivanc Sabirli,[4] Michael Davidson,[5] Matt Hilton,[6] Pedro T. P. Viana,[7,8] Chris A. Collins,[6] Scott T. Kay,[9] Andrew R. Liddle,[3] Robert G. Mann,[5] Christopher J. Miller,[10] Robert C. Nichol,[11] Michael J. West,[12,13] Christopher J. Conselice,[14] Hyron Spinrad,[15] Daniel Stern,[16] and Kevin Bundy[17]

Received 2006 March 31; accepted 2006 June 5; published 2006 July 14

ABSTRACT

We report the discovery of XMMXCS J2215.9−1738, a massive galaxy cluster at $z = 1.45$, which was found in the *XMM* Cluster Survey. The cluster candidate was initially identified as an extended X-ray source in archival *XMM* data. Optical spectroscopy shows that six galaxies within a ~60″ diameter region lie at $z = 1.45 \pm 0.01$. Model fits to the X-ray spectra of the extended emission yield $kT = 7.4^{+2.7}_{-1.8}$ keV (90% confidence); if there is an undetected central X-ray point source, then $kT = 6.5^{+2.6}_{-1.8}$ keV. The bolometric X-ray luminosity is $L_X = 4.4^{+0.8}_{-0.6} \times 10^{44}$ ergs s^{-1} over a 2 Mpc radial region. The measured T_X, which is the highest for any known cluster at $z > 1$, suggests that this cluster is relatively massive for such a high redshift. The redshift of XMMXCS J2215.9−1738 is the highest currently known for a spectroscopically confirmed cluster of galaxies.

Subject headings: galaxies: clusters: general — galaxies: evolution — galaxies: formation

1. INTRODUCTION

High-redshift galaxy clusters provide important laboratories for the study of structure formation and galaxy evolution. They also can be used to constrain cosmological parameters independent of the cosmic microwave background and supernova methods. The number of known clusters at $z > 1$ is currently small (≃10 with X-ray confirmation; e.g., Stanford et al. 2001, 2002; Rosati et al. 2004; Mullis et al. 2005), but growing rapidly thanks to new surveys being carried out in the X-ray (e.g., Romer et al. 2001; Mullis et al. 2005; Bremer et al. 2006; Barkhouse et al. 2006), optical (e.g., Gladders & Yee 2005), and infrared (e.g., Stanford et al. 2005). In the near future, Sunyaev-Zel'dovich surveys should also provide large numbers of high-redshift clusters (Carlstrom et al. 2002). We announce here the discovery of a high-redshift cluster in the *XMM* Cluster Survey (XCS; Romer et al. 2001) and the measurement of its X-ray temperature. At $z = 1.45$, XMMXCS J2215.9−1738 is the most distant cluster with spectroscopic redshift confirmation to date. Unless otherwise noted, we assume $\Omega_m = 0.27$, $\Lambda = 0.73$, and $H_0 = 70$ km s^{-1} Mpc^{-1}.

[1] University of California, Davis, CA 95616; adam@igpp.ucllnl.org.
[2] Institute of Geophysics and Planetary Physics, Lawrence Livermore National Laboratory, Livermore, CA 94551.
[3] Astronomy Centre, University of Sussex, Falmer, Brighton BN1 9QJ, UK.
[4] Department of Physics, Carnegie Mellon University, 5000 Forbes Avenue, Pittsburgh, PA 15217.
[5] Institute of Astronomy, University of Edinburgh, Blackford Hill, Edinburgh EH9 9HJ, UK.
[6] Astrophysics Research Institute, Liverpool John Moores University, Twelve Quays House, Egerton Wharf, Birkinhead CH41 1LD, UK.
[7] Departamento de Matemática Aplicada da Faculdade de Ciencias da Universidade do Porto, Rua do Campo Alegre 687, 4169-007 Porto, Portugal.
[8] Centro de Astrofisca da Universidade do Porto, Rua das Estrelas, 4150-762 Porto, Portugal.
[9] Astrophysics, Keble Road, Oxford OX1 3RH, UK.
[10] Cerro-Tololo Inter-American Observatory, National Optical Astronomy Observatory, 950 North Cherry Avenue, Tucson, AZ 85719.
[11] Institute of Cosmology and Gravitation, University of Portsmouth, Portsmouth PO1 2EG, UK.
[12] Department of Physics and Astronomy, University of Hawaii, 200 West Kawili Street, Hilo, HI 96720.
[13] Gemini Observatory, Casilla 603, La Serena, Chile.
[14] University of Nottingham, University Park, Nottingham NG9 2RD, UK.
[15] Astronomy Department, University of California, Berkeley, CA 94720.
[16] Jet Propulsion Laboratory, California Institute of Technology, MS 169-506, 4800 Oak Grove Road, Pasadena, CA 91109.
[17] California Institute of Technology, MS 105-24, 1200 California Boulevard, Pasadena, CA 91125.

2. OBSERVATIONS

2.1. *X-Ray*

XMM-Newton is the most sensitive X-ray spectral-imaging telescope deployed to date. The XCS identifies cluster candidates in the *XMM* data archive using the signature of X-ray extent. With a projected total area of 500 deg^2, the XCS is expected to catalog several thousand clusters out to a redshift of $z \simeq 2$ (Romer et al. 2001). To date, 1847 *XMM* observations have been processed using an automated pipeline, resulting in a survey area of 168 deg^2 at $b > 20°$. This is the net area available for cluster searching and excludes the Magellanic Clouds, artifacts due to out-of-time events, and X-ray sources that extend over a large fraction of the field of view, such as supernova remnants, Galactic clusters, or low-redshift galaxy clusters. The initial catalog contains 1764 cluster candidates (see M. Davidson et al. 2006 and K. Sabilri et al. 2006, both in preparation, for details). Here we focus on five moderately deep observations of varying length in the direction of the $z = 2.217$ quasar LBQS 2212−1759, which were obtained in 2000 and 2001. An extended source was detected at the 4 σ or greater level by the XCS pipeline at the same location, 9′ from the center of the field of view, in three of the five observations. The combined *XMM* exposure time, after correction for solar flares, etc., in the direction of the cluster candidate is 237 ks (MOS1). The typical point-source positional uncertainty in the XCS is 3″ at 9′ off-axis (M. Davidson et al. 2006, in preparation), and we have verified this by checking the positions of three quasars in the summed X-ray data near the cluster candidate.

2.2. *Optical and IR Imaging*

An *I*-band image of the area around XMMXCS J2215.9−1738 was found in the ESO Imaging Survey (Dietrich et al. 2006). This 9000 s image reaches a limiting magnitude

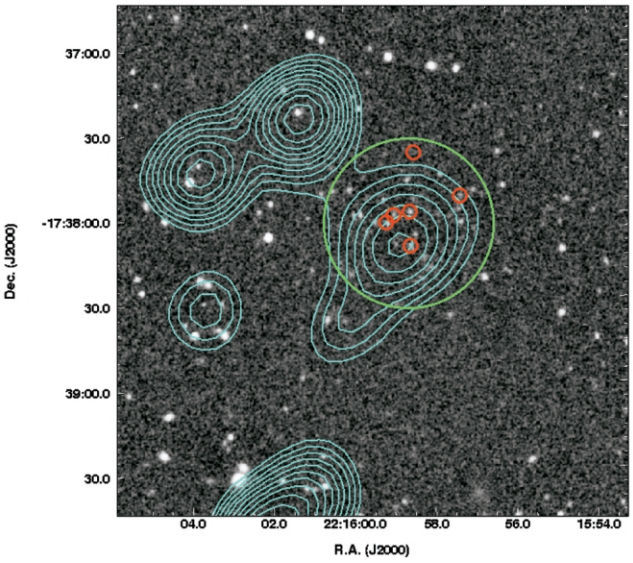

FIG. 1.—K_s-band image of a 3′ field centered on the cluster with an X-ray overlay of contours in blue. The six spectroscopically confirmed members are circled in red (ID = 14651 is not detected in the K_s image). The green circle of diameter 60″ shows the location of the region used for the X-ray analysis reported in § 3.1.

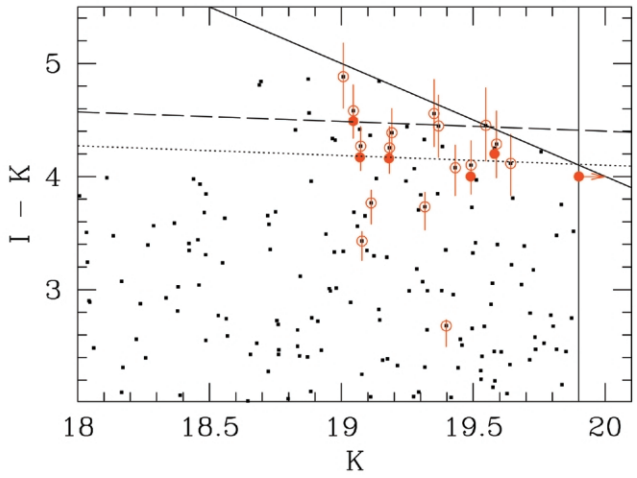

FIG. 2.—$I - K_s$ vs. K_s color-magnitude diagram for XMMXCS J2215.9−1738; aperture magnitudes are used for the colors and K_s magnitudes. The black points are all the objects within a 3′ box around the position of the X-ray source, and the objects circled in red lie within 30″ of the center of the X-ray source. The filled red circles are those with concurrent spectroscopic redshifts at $z = 1.45$. The dashed and dotted lines represents the expected color-magnitude relation for galaxies as predicted by a Bruzual & Charlot model in which all the stars formed within a 0.1 Gyr burst starting at $z_f = 3$ and $z_f = 2$, respectively, in the standard cosmology. The solid lines represent the 5 σ limits to the K_s and $I - K_s$ photometry.

of 24 (Vega), and allows even $z > 1$ early-type galaxies to be detected. On the basis of visual inspection of the *I*-band image, XMMXCS J2215.9−1738 was selected as a possible $z > 1$ galaxy cluster, worthy of spectroscopic follow-up.

Subsequent to the first slit mask spectroscopy (see below), K_s-band imaging was carried out on the 200 inch (5 m) telescope at Palomar on 2005 October 21. A total of 3240 s of exposure time was obtained in clear conditions, and the images were reduced following standard infrared procedures. The reduced image was calibrated onto the Vega system by comparison of instrumental magnitudes for stars with the same objects in the 2MASS database. The image is shown in Figure 1, along with contours of the X-ray emission. The X-ray emission from the cluster candidate is clearly extended compared to the three nearby point sources. None of the X-ray sources in Figure 1 (the cluster, the three point sources, or the southern extension) has been cataloged previously, based on an examination of the NED and SIMBAD databases.

The *I*- and K_s-band images were photometered using SExtractor. Objects were detected on the K_s image, and then aperture magnitudes of diameter 2.″5 were measured on both images using the same SExtractor catalog. The resulting color-magnitude diagram shown in Figure 2 was used for target selection for the second mask in the spectroscopic follow-up program.

2.3. *Keck Spectroscopy*

The first spectroscopic follow-up was carried out using the Deep Imaging Multi-Object Spectrograph (DEIMOS; Faber et al. 2003) at the Keck II telescope on UT 2005 September 1. Targets were selected from the *I*-band image to have $23 < I < 24$ and be located in the central few arcminutes of the area around the X-ray candidate cluster. The slits had widths of 1.″0 and minimum lengths of 5″. We used the 600ZD grating, which is blazed at 7500 Å, to cover a nominal wavelength range of 5000–10000 Å. The dispersion of ~0.65 Å pixel^{-1} resulted in a spectral resolution of 3.8 Å. Of particular note is that this spectral resolution is adequate for being able to detect both lines in the [O II] λ3727 doublet. We obtained 5 × 1800 s exposures with this setup in photometric conditions with 1.″1 seeing. The observations were carried out with the slitlets aligned close to the parallactic angle.

A second slit mask was observed, again using DEIMOS at the Keck II telescope, on UT 2005 November 5. For this mask, we were able to use the color information seen in Figure 2 to select targets likely to be in the cluster by choosing objects in the area of the color-magnitude diagram where the red sequence is expected for a $z = 1.45$ cluster. These observations were conducted in poor conditions, with ~1.″5 seeing. A total of 5400 s of exposure time was obtained with the second mask.

The slit mask data for the two masks were separately reduced using the DEEP pipeline. A relative flux calibration was obtained from long-slit observations of the standard stars G191B2B and Wolf 1346. One–dimensional spectra were extracted from the sum of the reduced data for each slitlet.

3. RESULTS

3.1. *X-Ray Analysis*

To examine the X-ray emission from the intracluster medium, we need to account for contamination from the nearby point sources. At the same time it behooves us to allow for a possible central point source, such as a galaxy with an active galactic nucleus, that would affect our attempts to extract information on, e.g., the temperature of the ICM. Using Sherpa, we carried out two-dimensional fitting of the detected nearby point sources simultaneously with fitting of the extended emission from the cluster candidate. In addition to the obvious point sources to the east of the cluster, we have included a variable-strength point source fixed at the center of the extended emission. The profile of the X-ray emission is shown in Figure 3. The best-fitting β-model combined with the point sources is shown, along with a PSF which indicates that extended emission is

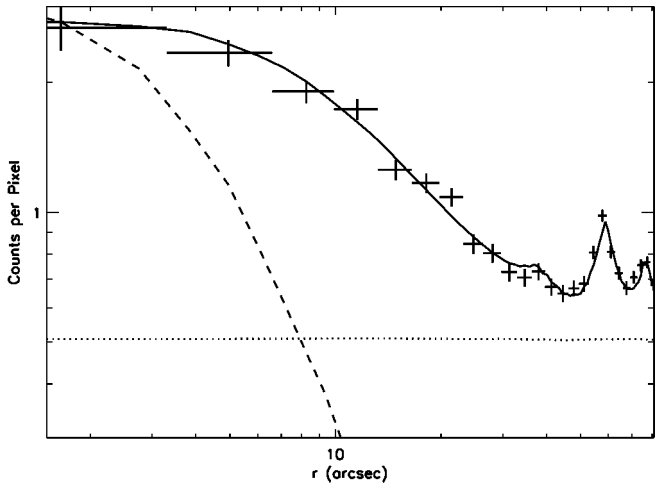

FIG. 3.—Spatial profile of the X-ray emission. The points are the data. The best-fitting model, combining both the extended component and the point sources (which are obvious as bumps at large radii), is shown by the solid line. A PSF is shown by the dashed line. The background is shown by the horizontal dotted line.

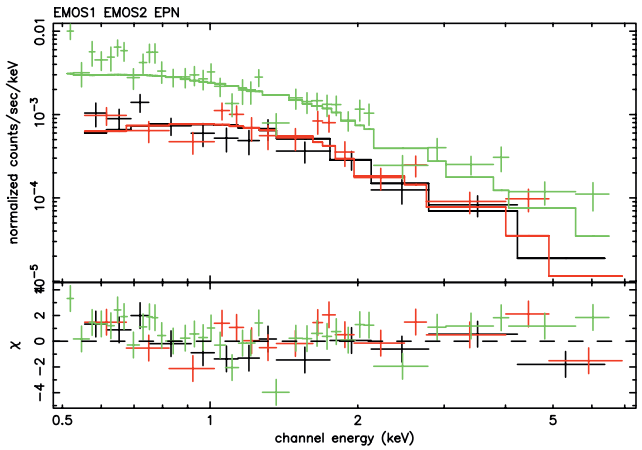

FIG. 4.—X-ray spectrum of XMMXCS J2215.9−1738. Counts from EMOS1, EMOS2, and EPN are plotted with black, red, and green, respectively. The spectra are after accounting for the point sources, including a possible central source. The best fit to these spectra is an absorbed MEKAL model with properties specified in the text; the folded model is overplotted (only T_X and the normalization are left as free parameters).

present. The brightest point sources are obvious as bumps in the profile at radii of ~37″, 60″, and 75″. We find that a central point source contributes at most 10% of the counts within the central $r = 30''$ region. The best-fitting β-model for the extended component has a core radius of $r_c = 73^{+18}_{-16}$ kpc and $\beta = 0.53^{+0.04}_{-0.03}$.

Next we used the results of this two-dimensional fitting procedure to accurately determine the spectrum of the extended emission after correction for contamination by the point sources. The appropriate counts due to the point sources were included (as fixed models normalized to the results of the spatial analysis) while carrying out the fitting of the extended source spectrum as described below. We have extracted a spectrum for the cluster candidate using photons detected within a 30″ radius of $\alpha = 22^h15^m58\overset{s}{.}5$, $\delta = -17°38'2\overset{''}{.}5$. We extracted MOS1, MOS2, and pn spectra from each *XMM* observation with an exposure time >10 ks made toward the cluster. We generated a combined spectrum for each camera, and these are presented in the top panel of Figure 4. Spectral fitting was carried out using XPSEC, version 11.3.1s (Arnaud 1996), using the MEKAL models (Mewe et al. 1986) modified with an interstellar absorption (McCammon & Sanders 1990) appropriate for the Galactic column density at that location. A local background correction was made using a spectrum extracted from a 30″ radius region at the same off-axis angle (9′) as the cluster; this avoids having to carry out an energy-dependent vignetting correction of the background. To find the best-fit spectrum, we limited the fit to the energy range 0.5–7 keV and grouped the data so that there were a minimum of 20 counts per bin. The number of background-corrected counts in that energy range (summed across all three cameras) was 1100 in the 30″ measurement aperture, after correction for the point sources. We fixed the hydrogen column density to the Dickey & Lockman (1990) value, the metal abundance to $Z = 0.3$ times the solar value, and, initially, the redshift to the Keck spectroscopic value, $z = 1.45$. After accounting for all point sources including the possible central source, the best-fit temperature of the extended emission was found to be $T_X = 6.5^{+2.6}_{-1.8}$ keV (90% confidence limits). If there is no central point source, then the best-fit temperature of the ICM would be $T_X = 7.4^{+2.7}_{-1.8}$ keV. The best-fit model and its residuals are shown in Figure 4. Using this spectrum, we have determined the cluster flux to be $1.22^{+0.21}_{-0.17} \times 10^{-14}$ ergs s^{-1} cm^{-2} (0.5–2.0 keV), extrapolated to a region 2 Mpc in radius using the best-fit β-model. For the same 2 Mpc aperture, the luminosity of the ICM is $1.15^{+0.20}_{-0.16} \times 10^{44}$ ergs s^{-1} in the 0.5–2.0 keV band, and $4.39^{0.76}_{-0.61} \times 10^{44}$ ergs s^{-1} in a bolometric band (0.05–100 keV).

3.2. *Optical Spectroscopy*

Visual inspection of the reduced spectra from both DEIMOS masks yielded redshifts for objects. The six galaxies listed in Table 1 lie within 30″ of the X-ray centroid and have concurrent redshifts $1.445 < z_{spec} < 1.455$. In three of the six spectra, the [O II] λ3727 doublet is detected and clearly split. The other three objects have spectra that show features from the redshifted 4000 and 2900 Å breaks. The spectrum of one of the cluster members, ID 14339, is shown in Figure 5. In addition to these six galaxies we consider to be members of the cluster, three more galaxies were spectroscopically identified with redshifts at $1.44 < z < 1.46$. However, they lie approximately 5′–7′ from the X-ray centroid, so are not (yet) clearly members of the cluster.

3.3. *Optical and Infrared Photometry*

The color-magnitude diagram for all objects in a 3′ area at the cluster is shown in Figure 2. The objects within 30″ of the X-ray centroid are circled in red. The six galaxies with concurrent spectroscopic redshifts $1.445 < z < 1.455$ are shown by

TABLE 1
SUMMARY OF SPECTROSCOPIC CLUSTER MEMBERS

ID	R.A. (J2000.0)	Decl. (J2000.0)	K_s	$I - K_s$	z_{spec}
14651	22 15 58.364	−17 37 37.5	>19.9	<4.0	1.4526
14478	22 15 57.233	−17 37 53.1	19.58	4.20	1.4537
14378	22 15 58.879	−17 37 59.6	19.49	4.00	1.451
14289	22 15 58.488	−17 38 10.4	19.04	4.49	1.453
14339	22 15 59.057	−17 38 02.0	19.18	4.16	1.4467
14389	22 15 58.479	−17 37 58.6	19.07	4.17	1.452

NOTE.—Units of right ascension are hours, minutes, and seconds, and units of declination are degrees, arcminutes, and arcseconds.

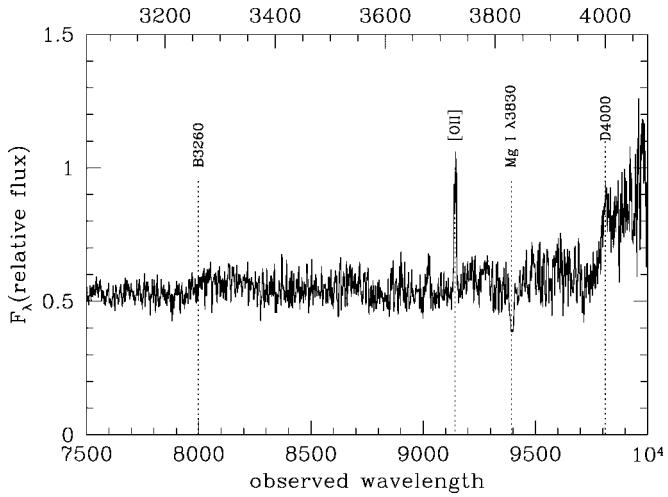

FIG. 5.—Optical spectrum of cluster member 14339 with $z = 1.45$. The identified spectral features are marked. The spectrum has been smoothed by a 6.5 Å boxcar.

the filled red circles. The scatter seen in the colors of the member galaxies is dominated by the photometric uncertainties in the photometry and so is not indicative of the intrinsic scatter in the red sequence in this cluster. Also plotted in Figure 2 are two estimates of the expected color of L^* early-type galaxies. Using a simple passive evolution model calculated from the GISSEL of Bruzual & Charlot (2003) and our assumed cosmology, we calculated the expected colors for a single 100 Myr burst stellar population of solar metallicity stars formed at $z_f = 3.0$ and $z_f = 2.0$, with slopes assumed to be the same as those in Coma for a similar rest-frame color. As can be seen in Figure 2, the colors of the member galaxies are consistent with those expected for early-type galaxies whose stars formed at $2 < z_f < 3.0$.

4. DISCUSSION

Analyses of our combined X-ray imaging spectroscopy, optical spectroscopy, and optical-IR imaging provide strong evidence that XMMXCS J2215.9−1738 is a massive galaxy cluster at $z = 1.45$. At least 10 galaxy clusters with $z > 1.4$ and $T_X > 6$ keV are expected to be present in our current XCS area of 168.2 deg^2, if the universe is assumed to be flat with $\Omega_m = 0.238$ and $\sigma_8 = 0.744$ (*WMAP*; Spergel et al. 2006). This estimate requires the relation between cluster mass and X-ray temperature to be normalized so as to reproduce the local abundance of X-ray clusters (HIFLUGCS; Reiprich & Böhringer 2002). However, it should be noted that these assumptions require that a local 5 keV cluster would need to have a mass, within an overdensity of 500 with respect to the critical density, of around $2 \times 10^{14}\, h^{-1}\, M_\odot$ (Pierpaoli et al. 2003; Viana et al. 2003), about two-thirds smaller than is implied by the most recent observational data (Arnaud et al. 2005; Vikhlinin et al. 2006).

With the combination of the serendipitous searches for clusters in the *XMM* archival data (Romer et al. 2001; Mullis et al. 2005) and the ongoing wide-area surveys such as UKIDSS (A. Lawrence et al. 2006, in preparation) and the RCS (Gladders & Yee 2005), the time finally is ripe for the identification of large samples of $z > 1$ clusters. The construction of such samples will pave the way toward a better understanding of the origin of galaxy clusters and their constituent galaxy populations.

This work is based on data obtained by *XMM-Newton*, an ESA science mission funded by contributions from ESA member states and from NASA. We acknowledge financial support from the NASA-LTSA program, the RAS Hosie Bequest, Liverpool John Moores University, the Institute for Astronomy at the University of Edinburgh, the *XMM* and *Chandra* guest observer programs, Carnegie Mellon University, the NSF, and PPARC. This research made use of the NASA/IPAC Extragalactic Database, the SIMBAD facility at CDS, the NASA/GSFC-supported XSPEC software, and the ESO Imaging Survey. The W. M. Keck Observatory is a scientific partnership between the University of California and the California Institute of Technology, made possible by a generous gift of the W. M. Keck Foundation. The authors wish to recognize and acknowledge the very significant cultural role and reverence that the summit of Mauna Kea has always had within the indigenous Hawaiian community; we are fortunate to have the opportunity to conduct observations from this mountain. The analysis pipeline used to reduce the DEIMOS data was developed at UC Berkeley with support from NSF grant AST 00-71048. We thank the referee for helping to improve the final version of this paper. The work by S. A. S. at LLNL was performed under the auspices of the US Department of Energy under contract W-7405-ENG-48. The work of D. S. was carried out at the JPL, California Institute of Technology, under contract with NASA.

REFERENCES

Arnaud, K. 1996, in ASP Conf. Ser. 101, Astronomical Data Analysis Software and Systems V, ed. G. Jacoby & J. Barnes (San Francisco: ASP), 17
Arnaud, M., Pointecouteau, E., & Pratt, G. W. 2005, A&A, 441, 893
Barkhouse, W. A., et al. 2006, ApJ, in press
Bremer, W., et al. 2006, MNRAS, in press
Bruzual A., G., & Charlot, S. 2003, MNRAS, 344, 1000
Carlstrom, J. E., Holder, G. P., & Reese, E. D. 2002, ARA&A, 40, 643
Dickey, J. M., & Lockman, F. J. 1990, ARA&A, 28, 215
Dietrich, J. P., et al. 2006, A&A, 449, 837
Faber, S., et al. 2003, Proc. SPIE, 4841, 1657
Gladders, M., & Yee, H. 2005, ApJS, 157, 1
McCammon, D., & Sanders, D. T. 1990, ARA&A, 28, 657
Mewe, R., Lemen, J. R., & van den Oord, G. H. J. 1986, A&AS, 65, 511
Mullis, C., et al. 2005, ApJ, 623, L85
Pierpaoli, E., Borgani, S., Scott, D., & White, M. 2003, MNRAS, 342, 163
Reiprich, T. H., & Böhringer, H. 2002, ApJ, 567, 716
Romer, K., Viana, P. T. P., Liddle, A. R., & Mann, R. G. 2001, ApJ, 547, 594
Rosati, P., et al. 2004, AJ, 127, 230
Spergel, D. N., et al. 2006, ApJ, submitted (astro-ph/0603449)
Stanford, S. A., Holden, B., Rosati, P., Eisenhardt, P., Stern, D., Squires, G., & Spinrad, H. 2002, AJ, 123, 619
Stanford, S. A., et al. 2001, ApJ, 552, 504
———. 2005, ApJ, 634, L129
Viana, P. T. P., Kay, S. T., Liddle, A. R., Muanwong, O., & Thomas, P. A. 2003, MNRAS, 346, 319
Vikhlinin, A., Kravtsov, A., Forman, W., Jones, C., Markevitch, M., Murray, S. S., & Van Speybroeck, L. 2006, ApJ, 640, 691